Direct numerical simulation study of the interaction between the polymer effect and velocity gradient tensor in decaying homogeneous isotropic turbulence*

Cai Wei-Hua(蔡伟华)†, Li Feng-Chen(李凤臣)‡, and Zhang Hong-Na(张红娜)

School of Energy Science and Engineering, Harbin Institute of Technology, Harbin 150001, *China*

(Received 4 June 2011; revised manuscript received 13 July 2011)

Direct numerical simulation of decaying homogeneous isotropic turbulence (DHIT) of a polymer solution is performed. In order to understand the polymer effect on turbulence or additive-turbulence interaction, we directly investigate the influence of polymers on velocity gradient tensor including vorticity and strain. By visualizing vortex tubes and sheets, we observe a remarkable inhibition of vortex structures in an intermediate-scale field and a small-scale field but not for a large scale field in DHIT with polymers. The geometric study indicates a strong relevance among the vorticity vector, rate-of-strain tensor, and polymer conformation tensor. Joint probability density functions show that the polymer effect can increase "strain generation resistance" and "vorticity generation resistance", i.e., inhibit the generation of vortex sheets and tubes, ultimately leading to turbulence inhibition effects.

Keywords: decaying homogeneous isotropic turbulence, turbulent drag-reducing flow, velocity gradient tensor, direct numerical simulation

PACS: 47.27.ek, 47.27.Gs, 47.32.C–, 47.50.–d **DOI:** 10.1088/1674-1056/20/12/124702

1. Introduction

The turbulent drag reduction by a small quantity of polymer additives was first reported by Toms[1] in 1949, and the drag-reducing effect of polymers was thus named "the Toms effect". Since then, the turbulent characteristics and physical mechanism of drag reduction (DR) by additives have been intensively investigated in channel, pipe, and boundary-layer flows through theoretical analyses,[2,3] experiments,[4−6] and numerical simulations[7,8] due to the wall-bounded natures of those flow geometries. The phenomenon analogous to DR in wall-bounded turbulent flow, i.e. turbulence inhibition, also occurs in flows away from the wall such as grid turbulence (or isotropic turbulence)[9−16] and bulk turbulence[17−21] of drag-reducing solutions, which were interpreted based on elastic theory.[22,23] Note that the nomenclature "drag reduction" has also been used for turbulent flows without the wall effect.[12,20,21,24] Since drag is usually connected with a solid-wall-fluid interface, in order to avoid confusion, we rephrase "drag reduction or drag-reducing effect" for isotropic turbulence as "turbulence inhibition or turbulence-inhibiting effect" herein. By comparison with wall-bounded turbulence, the most remarkable advantage of homogeneous isotropic turbulence (HIT) is that there is no mean shear, hence polymers cannot change the momentum flux but can change the energy flux from large to small scale. Therefore, the study on HIT with drag-reducing additives is of fundamental importance for studying the interactions between turbulence and drag-reducing additives and understanding its physical mechanism. To understand the mechanism of how drag-reducing additives influence turbulent structure and turbulent kinetic energy cascading in decaying homogeneous isotropic turbulence (DHIT) with polymer additives, we have carried out direct numerical simulation (DNS) for Newtonian fluid and polymer solution cases. In our previous numerical studies on DHIT,[24] we found that (i) with polymer additives the decay of turbulent kinetic energy is faster than that in the Newtonian fluid case; (ii) the classical Kolmogorov energy cascade is modified due to the release of the polymer elastic energy into flow structure on a small scale in the polymer solution case; (iii) both the enstrophy

*Project supported by the National Natural Science Foundation of China (Grant No. 10872060) and the Fundamental Research Funds for the Central Universities (Grant No. HIT.BRET2.2010008).

†E-mail: caiwh@hit.edu.cn

‡Corresponding author. E-mail: lifch@hit.edu.cn

© 2011 Chinese Physical Society and IOP Publishing Ltd

and the strain are smaller than those in the Newtonian fluid case and the polymer effect on these two variables is negative. According to our analysis, we proposed an intuitive and natural definition for evaluating the turbulence inhibiting effect by polymer additive (we used the terminology of "drag reduction" in that paper) in DHIT based on the statistical kinetic energy decay, different from those in Kalelkar *et al.*[20] and Perlekar *et al.*[21]

To study the dynamics of turbulence, we can investigate the dynamics of velocity gradient. In comparison with velocity, the field of the velocity gradient is much more sensitive to the non-Gaussian nature of turbulence or more generally to its structure, and hence reflects more of its physics. It is also a Galilean invariance containing significant fluid mechanical information independent of the reference of a moving observer. Moreover, its dynamical behaviour governs the mechanism of vortex stretching which in turn contributes to the energy cascade process in turbulent flows (as pointed out by Sagaut and Cambon:[25] "The turbulent kinetic cascade in Fourier space must be replaced with the generation of velocity gradients (i.e., both vorticity and strain) in physical space.)". Therefore, its evolution is of primary importance in the understanding of the kinematics and dynamics of turbulence. The velocity gradient includes two parts: vorticity, and strain. Taylor[26] pointed out the importance of vorticity in 1937, and the role of strain was emphasized by Kolmogorov[27] in 1941. Tennekes and Lumley[28] argued that vortex stretching is the physical mechanism leading to the hypothesized energy cascade from large to small scales. However, Tsinober[29] noted that in physical space the mechanism of the energy cascade is not due to vortex stretching but due to vortex compression which contributes to large strain generation. He also emphasized the importance of strain (as pointed out by Kolmogorov in 1941) as well as vorticity in the context of creation and maintenance of turbulence. These two quantities should be considered in parallel, as they are weakly correlated in isotropic turbulence but tied by a strongly nonlocal relation.[25]

Up to now, based on the velocity gradient (i.e., both vorticity and strain) much attention has been paid to vortex structures, topological dynamics, geometric study direct vorticity, and strain fields, etc. Several coherent structures have been identified, such as, vortex 'worms' or 'filament' in isotropic turbulence,[30−32] vortex 'braids' in turbulent shear layers,[33] quasi-streamwise vortices,[34] and 'hairpin' vortices in wall turbulence.[35] By these observations, it is confirmed that these typical vortex structures are the dominant structures in turbulent flows. The structure and the evolution for velocity gradient are also studied based on the topological approach introduced by Chong *et al.*[36] by not studying these tensors directly but investigating their invariants (the second and third invariants of the velocity gradient tensor, i.e., Q and R, respectively). This method was first used by Chen *et al.*[37] to study turbulent compressible and incompressible mixing layer flows and now is extensively used in isotropic turbulence,[38,39] turbulent mixing layer,[40] and turbulent channel flows.[41] Alignments are suited for events of any magnitude, since they do not contain the amplitudes of quantities involved. Alignments are invariant in the sense that they are independent of the reference system and therefore, along with other invariant quantities are most appropriate in studying physical processes generally and in particular for the structural nature of turbulent flows.[42] Ashurst *et al.*[43] first found that the vorticity vector tends to be aligned with the intermediate eigenvector of rate-of-strain tensor and that strain in this direction is mostly positive for isotropic flow and homogeneous shear flow. This phenomenon has been proved in isotropic turbulence from numerical[44] and experimental results[45] and also in boundary layer flow.[45] Jiménez[46] showed that this vorticity-intermediate eigenvector alignment is an expected kinematic consequence of the presence of vortex tubes. Besides, Tsinober *et al.*[45] found that there is a strong tendency towards the alignment between the vorticity vector and vortex stretching vector in the strict sense, i.e. a tendency towards their being parallel but not antiparallel. This result along with the positiveness of the enstrophy generation term is the manifestation of the strong non-Gaussianity of the field of velocity gradient.

For turbulent flows with polymer additives, owing to its elastic nature the presence of polymers significantly modifies the turbulent characteristics relative to the Newtonian fluid flows, such as energy cascade, behaviour of vortical structures, intermittency, etc, leading to DR. According to the role of velocity gradient, it is of fundamental importance to study the polymer effect on the parameters of vorticity and strain and to understand the modification produced by additives–turbulence interaction and the DR mechanism. Some studies have been carried out through in-

vestigating the vortical structures generated in turbulent channel flow and HIT. The experimental results of Kawaguchi *et al.*[47] in turbulent channel flow showed that for water flow, "streaming" structures are the largest contributor among the four kinds of vortical structures and only in the near-wall thin layer can the probability of "shear" structure becomes the largest. In contrast, drag-reducing surfactant solution flow has a thick layer characterized by "shear" structure, where the probabilities of "eddies" and "convergence" structures become small. Kim *et al.*[48] found that the near-wall vortical structures are weakened and elongated in the streamwise direction by the polymer stress and the three-dimensional distributions of conditionally averaged polymer force around these vortical structures showed that the polymer force components oppose the vortical motion. Kim and Sirviente[49] argued that the polymer structures can contribute to minimizing the interaction between the inner and outer regions of flow, which in turn, can contribute to the modification of turbulent coherent structures through a detailed analysis of experimental data obtained using laser Doppler velocimetry. The DNS results of Sibilla and Beretta[50] showed that the mean vortex near wall is weaker, less tilted and inclined, while its length and radius are larger based on the Jeong and Hussain's vortex identification criterion.[51] Recently, proper orthogonal decomposition was used for analysing coherent structures in drag-reducing turbulent channel flows, suggesting that the basic shape and strength of coherent structures existing in CTAC (a kind of drag-reducing surfactant additive) solution flow are more regular and weaker, respectively, than those existing in water flow.[52,53] In DHIT the numerical results of De Angelis *et al.*[19] and Perlekar *et al.*[21] showed a decrease of small-scale vorticity filaments and our previous study results also proved this phenomenon.[24] Except for investigating the vortical structures, researches have also been directly devoted to the field of velocity gradient. Gyr and Tsinober[54] studied the behaviour of velocity gradient $\partial u_1/\partial x_1$ (x_1-streamwise coordinate) in channel flows and obtained that both $\langle(\partial u_1/\partial x_1)^2\rangle$ and $\langle(\partial u_1/\partial x_1)^3\rangle$ are an order of magnitude smaller in drag-reducing turbulent flows of polymer and surfactant solutions than those in pure water. Crawford *et al.*[15] addressed the influence of polymer on some statistical properties of the Lagrangian accelerations, which include a decrease in acceleration variance and an increase in the smallest time scale. Liberzon *et al.*[13] investigated the relationship between vorticity vector and rate-of-strain tensor including the angle between vorticity vector and vortex stretching vector, and the angle between vorticity vector and the first eigenvector of the rate-of-strain tensor in bulk turbulence using three-dimensional particle tracking velocimetry. The results showed that these angles are weak at later time in polymer solution flow compared with the flow of pure water. Besides, they found that the typical teardrop shape of Q–R topological map remained practically unchanged, but stressed that the reduced values of strain, enstrophy, and their production co-occur in the region of the teardrop "tail".[14]

Recently, Watanabe and Gotoh[55] investigated the statistical properties and the dynamics of ensembles of polymers in isotropic turbulence from the mean, variance, autocorrelation time and probability density function (PDF) of the end-to-end vector distance. The studies indicated that there exists the Weissenberg number effect on the coil-stretch transition and the alignment of the end-to-end vector versus the principal axis of rate-of-strain.

These important previous studies mainly focused on the consequences of introducing the polymer additives such as the modification of vortical structures and energy cascade, the change of some important parameters, and so on. We believe that in order to understand the polymer effect or additive–turbulence interaction, it is also necessary to build some relation between turbulence characteristics and polymer conformation field. On the other hand, the relation possibly leads to some new understandings and methods of sub-grid modeling for turbulent drag-reducing flows. So in the present paper, we mainly investigate the relation and interaction between polymer conformation field and vorticity/strain fields. The rest of the present paper is organized as follows. In Sections 2 and 3, numerical methods used in the simulations and vortex identification methods are briefly introduced, respectively. Then we show the results and analyses on the basis of vortex structure visualization and the interaction between polymer conformation and vorticity/strain fields in Section 4. Finally, we draw some conclusions and make discussion in Section 5.

2. Numerical methods

DNS for incompressible fluid with and without polymer additives have been carried out based on the Navier–Stokes (N–S) equation coupled with the

finitely extensible nonlinear elastic Peterlin (FENE-P) model.

The governing equations for DHIT of polymer solutions are as follows:[24]

$$\partial \boldsymbol{u}/\partial t + \boldsymbol{u}\cdot\nabla\boldsymbol{u} = -\nabla p/\rho + \nabla\cdot\boldsymbol{T}^{[s]}/\rho + \nabla\cdot\boldsymbol{T}^{[p]}/\rho, \quad (1)$$

$$\partial \boldsymbol{C}/\partial t + \boldsymbol{u}\cdot\nabla\boldsymbol{C} = \boldsymbol{C}\cdot\nabla\boldsymbol{u} + \nabla\boldsymbol{u}^{\mathrm{T}}\cdot\boldsymbol{C} - \left(f(r)\boldsymbol{C}-\boldsymbol{I}\right)/\tau_{\mathrm{p}}, \quad (2)$$

where $\boldsymbol{u}(\boldsymbol{x},t)$ is the velocity vector, $p(\boldsymbol{x},t)$ the local pressure, ρ the fluid density, $\boldsymbol{T}^{[s]} = 2\rho\upsilon^{[s]}\boldsymbol{S}$ the viscous stress due to the solvent, $\upsilon^{[s]}$ the solvent kinematic viscosity, $\boldsymbol{S} = (\nabla\boldsymbol{u} + \nabla\boldsymbol{u}^{\mathrm{T}})/2$ the rate-of-strain tensor, $\nabla\boldsymbol{u} = \partial u_i/\partial x_j$, $\nabla\boldsymbol{u}^{\mathrm{T}} = \partial u_j/\partial x_i$, $\boldsymbol{T}^{[p]} = \rho\upsilon^{[p]}\left(f(r)\boldsymbol{C}-\boldsymbol{I}\right)/\tau_{\mathrm{p}}$ the elastic stress due to polymer additives, $\upsilon^{[p]}$ the polymer kinematic viscosity, τ_{p} the polymer relaxation time, and C_{ij} the conformation tensor. In the FENE-P model, $f(r) = \left(L^2-3\right)/\left(L^2-r^2\right)$ ensures the finite extensibility, $r^2 = \mathrm{trace}(\boldsymbol{C})$ and L ($L = 100$ in our simulations) are the extension length and the maximum possible extension of polymer, respectively.

To solve Eq. (1), a standard pseudo-spectral code with 96^3 collocation points in the periodic cubic domain of size $l = 2\pi$ cm is used for spatial discretization[56,57] with all the nonlinear terms fully de-aliased by the 3/2 rule. A second-order Adams–Bashforth scheme is adopted for time advancement. To solve Eq. (2), for spatial discretization a second-order central difference scheme is used except for the convective term using the second-order Kurganov–Tadmor (KT) scheme[58] and for time marching a second-order Adams–Bashforth scheme is adopted. Initial turbulent kinetic energy spectrum $E_0(k) = 0.01k^4\exp(-0.14k^2)$ is adopted, where k is the wavenumber and the divergence-free initial velocity field $\hat{u}_0(\boldsymbol{k})$ is generated in Fourier space according to Rogallo's procedure.[56] The variable with the hat "$\wedge$" represents that it is in Fourier space. For initial conformation field, $C_{ij}^0(x,y,z) = \delta_{ij}$, polymers are assumed to be non-stretched.[21] The Taylor Reynolds number Re_λ and the Weissenberg number Wi are defined as $Re_\lambda = \sqrt{20}\xi^{N,m}/\sqrt{3\upsilon^{[s]}\varepsilon^{N,m}}$, $Wi{=}\tau_{\mathrm{p}}\sqrt{\varepsilon^{N,m}/\upsilon^{[s]}}$, respectively, where $\xi^{N,m}$ and $\varepsilon^{N,m}$ are the total kinetic energy and the energy-dissipation rate for the Newtonian fluid case at $t = t_m$, respectively.[21] In our previous studies,[24] we investigated different values of τ_{p} and β in numerical simulations and found that there exists a maximum drag reduction effect when τ_{p} and β are 0.1 and 0.6, respectively. So in this paper, the basic parameters are as follows: $Re_\lambda = 26.2$, $Wi = 0.62$, $\tau_{\mathrm{p}} = 0.1$ s, $\beta = 0.6$ (a dimensionless measure of polymer solution concentration, and smaller β corresponds to denser polymer solution) for polymer solution case and $Re_\lambda = 26.2$ for the Newtonian fluid case. In this paper, we choose DNS data at three sequential instants at $t = 0.6$ s (at which the enstrophy for the Newtonian fluid case reaches a maximum value), 2.0 s and 5.0 s (in the energy decaying period). The detailed description of numerical simulations can be found in Ref. [24].

3. Multi-scale method of identifying vortex structure

The existence of coherent structures is one of the most important characteristics in turbulence, and coherent structures can be divided into two groups: one has a tubular or filamentary structure (tube-like structure or vortex tube) and the other has a non-filamentary vorticity distribution (sheet-like structure or vortex sheets), each of which undoubtedly plays an important role in the overall dynamics and kinematics of turbulence. As for vortex sheets the most prominent characteristic is that in the region where strain and vorticity are highly correlated with each other and comparably equal in their magnitudes, and considerable dissipation of turbulent kinetic energy which is the final result of energy cascade takes place. In a polymer solution flow the introduction of polymer additives can significantly modify the behaviour and properties of coherent structure, which is closely related to the physical mechanism for turbulent drag-reducing flow. Extracting coherent structures from a turbulent field is a fundamental way to investigate the characteristics of coherent structure.

During the visualization of vortex tubes, several methods have been considered based on the second invariant (Q), discriminant (Δ) or eigenvalues (λ_2, λ_{ci}) of velocity gradient tensor ($\nabla\boldsymbol{u}$),[51,59–61] which have been widely used in the Newtonian fluid turbulent flows, such as isotropic turbulence,[62] channel flow,[63] mixing layer, and backward-facing step flow.[64] For viscoelastic flows, Sibilla and Beretta[50] investigated the near-wall coherent structures in a turbulent channel flow using λ_2 criterion. In HIT with polymer additives, Angelis *et al.*[19] and Perlekar *et al.*[21] studied tube-like structures by Δ and vorticity $|\boldsymbol{\omega}|$ criterions,

respectively. In our paper, we use the second invariant Q method, which is shown as follows.

Three invariants for velocity gradient tensor $\nabla \boldsymbol{u}$ are introduced as

$$\begin{aligned} P &= S_{ii}P = S_{ii}, \quad Q = \left(P^2 - S_{ij}S_{ji} - W_{ij}W_{ji}\right)/2, \\ R &= (-P^3 + 3PQ - S_{ij}S_{jk}S_{ki} \\ &\quad - 3W_{ij}W_{jk}W_{ki})/3, \end{aligned} \tag{3}$$

where $S_{ij} = (\partial u_i/\partial x_j + \partial u_j/\partial x_i)/2$ is the rate-of-strain tensor and $W_{ij} = (\partial u_i/\partial x_j - \partial u_j/\partial x_i)/2$ is the rate-of-rotation tensor.

For the incompressible flow,

$$\begin{aligned} &P = 0, \quad Q = (W_{ij}W_{ij} - S_{ij}S_{ij})/2, \\ &R = (-S_{ij}S_{jk}S_{ki} - 3W_{ij}W_{jk}W_{ki})/3. \end{aligned} \tag{4}$$

The second invariant Q reflects the relative strengths of rotation and strain. The first term on the right-hand side of Q expression in Eq. (4) is proportional to enstrophy density and the second term is proportional to dissipation rate. The positive Q isosurface isolates the areas where the strength of rotation is larger than that of strain, thus a tube zone can be defined as a region with the positive Q isosurface.[59,61]

However, unlike vortex tubes, very few identification methods[65,66] for vortex sheets have been proposed because vortex sheets are more disorganized than vortex tubes and susceptible to small disturbances, which makes it fairly difficult to be examined in turbulent flows. Recently, Horiuti and Takagi[67] proposed a new definition based on the eigen-decomposition of symmetric second-order velocity gradient tensor, $A_{ij} = S_{ik}W_{kj} + S_{jk}W_{ki}$, for vortex sheets. Since $A_{ii} = 0$, the eigenvalues of A_{ij} are obtained from the equation:

$$x^3 - (A_{ij}A_{ji})x/2 - A_{ij}A_{jk}A_{ki}/3 = 0. \tag{5}$$

Then, let $[A_{ij}]_z$, $[A_{ij}]_+$, and $[A_{ij}]_-$ denote the eigenvalue associated with the eigenvector that is maximally aligned with the velocity vector, the largest remaining eigenvalue, and the smallest eigenvalue, respectively. It is observed that vortex sheets can be examined based on the criterion:

$$[A_{ij}]_+ > \{[A_{ij}]_+\}_{\rm th}, \tag{6}$$

where $\{[A_{ij}]_+\}_{\rm th}$ is an arbitrary positive threshold. In this paper, we use this method (hereinafter it is referred to as H-T method) to identify vortex sheets in DHIT.

Usually, applying the above vortex-identifying methods to the whole flow field, the results have a tendency to show only vortex structures in the whole flow field. So the characteristics of vortex structure in a large-scale field and an intermediate-scale field can be difficult to study. Firstly, the velocity field is transformed into Fourier space by fast Fourier transformation, then the high frequency components are removed at two different thresholds and finally returned to physical space.[68] The velocity field ($t = 0.6$ s) is filtered in Fourier space by different cut-off frequencies:

$$u(x) = \sum_{|k| \le k_c} \hat{u}(k)\, {\rm e}^{{\rm i}\, kx}, \tag{7}$$

where all modes greater than the cut-off wavenumber k_c are set to be zero. In our study, the flow field is divided into three parts of different scales: large-scale field ($0 < k \le 4$), intermediate-scale field ($0 < k \le 8$), and small-scale field (the whole flow field). The energy spectrum is calculated for each scale field using the same energy spectrum function.

4. Results and discussion

4.1. Multi-scale coherent structure visualization

We first visualize vortex tubes and sheets in three fields with different scales for DHIT at $t = 0.6$ s with and without polymers based on Q criterion[59,61] and H-T method,[66] respectively, as shown in Figs. 1 and 2. Usually different choices of the threshold value change the appearance of vortex structure, for instance, raising the threshold value too high will result in losing some important vortices and setting the threshold value too low will cause an unclear visualization. Such a threshold value is chosen that a large number of vortices can be visualized and at the same time different vortices are distinguishable.[62] In the present paper, the isosurface of Q and $[A_{ij}]_+$ with a threshold $Q_{\rm th} = 2Q'_{\rm rms}$ and $\{[A_{ij}]_+\} = 2\{[A_{ij}]_+\}'_{\rm rms}$, where $Q'_{\rm rms}$ and $\{[A_{ij}]_+\}'_{\rm rms}$ are the average root mean squares of the Q and the $[A_{ij}]_+$ fluctuations, respectively.

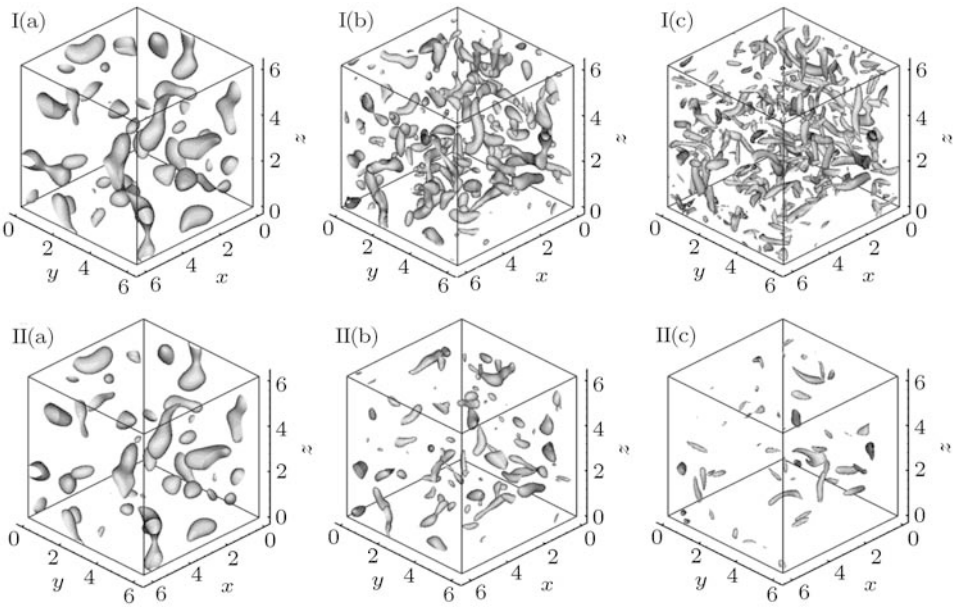


Fig. 1. Constant Q isosurface for I Newtonian case and II polymer solution case in the fields with three different scales i.e., (a) large-scale filed ($Q = 0.9141$), (b) intermediate-scale field ($Q = 4.6695$), and (c) small-scale field ($Q = 9.4685$).

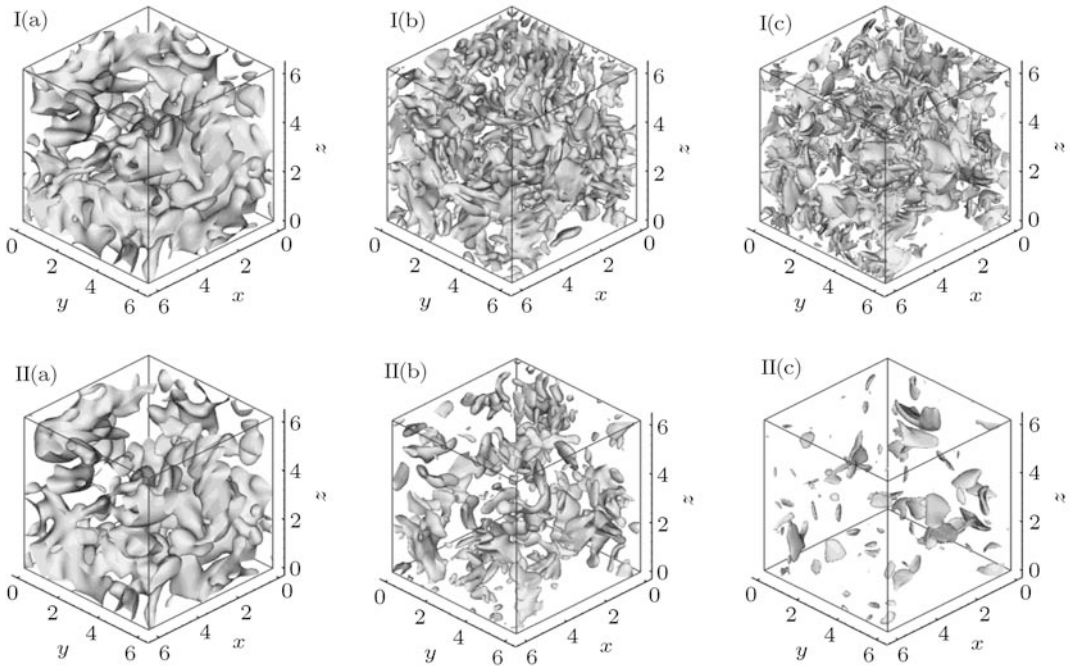


Fig. 2. Constant $[A_{ij}]_+$ isosurface for I Newtonian case and II polymer solution case in three fields with different scales, i.e., (a) large-scale field ($[A_{ij}]_+ = 0.6682$), (b) intermediate-scale field ($[A_{ij}]_+ = 3.6454$), and (c) small-scale field ($[A_{ij}]_+ = 11.2406$).

As is known, vortex structures play an essential role in turbulence dynamics such as the generation of turbulence, and the enhancement of the transport of mass, momentum and kinetic energy of fluid. From Figs. 1 and 2, a remarkable decrease of vortex tubes and sheets in intermediate-scale and small-scale fields can be observed in DHIT with polymer as compared with the Newtonian fluid case. Nonetheless, in the large-scale field the inhibition effect by polymers is not so distinct as that in other scale fields. In the vortex sheet region the polymer effect is the most dominant since the distribution of the polymer elastic energy is primarily concentrated along vortex sheets (as interpreted in Subsubsection 4.2.1), which finally results in a depression of vortex sheets in intermediate-scale and small-scale fields as shown in Fig. 2II. In the vortex

tubes region, the polymer effect also plays an inhibiting role in its generation (as interpreted in Subsubsection 4.2.2). At other instants the same phenomena are found and not shown here for brevity. It is known that the formation of a vortex tube is generally attributed to rolling-up of a single sheet due to Kelvin–Helmholtz instability, but Horiuti *et al.*[69] argued that a vortex tube is formed through the interaction between two different vortex sheets. The depression of vortex sheets (as shown in Fig. 2II) will cause the decrease of the interaction frequency between two different vortex sheets, thus preventing the sheet-tube transformation. As pointed out by Horiuti *et al.*:[69] "By terminating an occurrence of this sheet-tube transformation and subsequent energy cascade, the turbulence generation may be annihilated", when polymers are introduced into the flow, turbulence generation is inhibited (also interpreted in Subsubsections 4.2.1 and 4.2.2). What is more, vortex tubes and sheets are also very important for energy dissipation and cascade. Their depression especially in intermediate-scale and small-scale fields, implies the decrease of dissipation rate and modification of energy cascade to some extent.[24]

4.2. Interactions between strain rate, vorticity, and polymers

4.2.1. Interactions between polymer conformation and strain field

The above visualization of vortex structures exhibits a remarkable inhibition effect on both vortex tubes and sheets by polymers, especially in the small-scale field. As introduced before, the rate-of-strain tensor is a very important parameter in investigating vortex sheets, and it directly relates to the dissipation rate. Moreover, the development of small-scale turbulence highly relies on the evolution of rate-of-strain tensor, and in particular on the behaviour of the intermediate eigenvalue and its associated eigenvector. Here, it is found that for the turbulence with polymers, the characteristics of turbulence such as vortex sheets, dissipation, and development of small-scale motions are markedly inhibited. So, to understand the inherent mechanism produced by polymers, in the present paper we directly investigate the interactions between polymer conformation field and strain field.

Let $\boldsymbol{e}_i$ (i = 1, 2, 3) denote the three eigenvectors of rate-of-strain tensor $\boldsymbol{S}$ and α_i (i = 1, 2, 3) represent the corresponding eigenvalues reordered so that $\alpha_1 \geq \alpha_2 \geq \alpha_3$ which can be regarded as the strength of strain in the corresponding direction determined by $\boldsymbol{e}_i$. The incompressibility constraint yields $\alpha_1 + \alpha_2 + \alpha_3 = 0$, meaning that there is at least one positive eigenvalue (α_1) and one negative eigenvalue (α_3). However, the intermediate eigenvalue α_2 can be either negative or positive, and it is a very important parameter to determine whether the local flow structure is tube-like ($\alpha_2 < 0$) or sheet-like ($\alpha_2 > 0$).[70] Then, PDFs of these eigenvalues at $t = 0.6$ s for both the Newtonian fluid and polymer solution cases are shown in Fig. 3. For polymer solution case PDFs values of three eigenvalues are all reduced in the regions of large eigenvalues, i.e. large strain, but increased in the regions of small eigenvalues, i.e. small strain as compared with its Newtonian counterpart. It indicates that the ensemble strength of the strain in each direction is weakened by polymers. Moreover, for both the Newtonian fluid case and the polymer solution case the intermediate eigenvalue (α_2) is positively skewed, adequately suggesting that most regions (two positive eigenvalues) in the flow field are vortex sheets.[70] At other instants the same phenomena are found and not shown here for brevity. From this viewpoint it shows the importance of vortex sheets for both the Newtonian fluid case and the polymer solution case. Similarly, let $\boldsymbol{a}_i$ (i = 1, 2, 3) denote three eigenvectors of polymer conformation tensor reordered by the magnitudes of three eigenvalues (λ_i, i = 1, 2, 3, $\lambda_1 > \lambda_2 > \lambda_3$). Here, λ_i (i = 1, 2, 3) shows the strength of polymer deformation in the corresponding direction $\boldsymbol{a}_i$ (i = 1, 2, 3), respectively, and their PDFs at $t = 0.6$ s are shown in Fig. 4. It is obtained that $\lambda_1 > 1$ and $\lambda_3 < 1$, i.e., polymers are stretched and coiled in the directions of $\boldsymbol{a}_1$ and $\boldsymbol{a}_3$, respectively. But λ_2 can be either $\lambda_2 > 1$ or $\lambda_2 < 1$, determined by the local flow motions. Under the simulating conditions, it is found that λ_2 is skewed at $\lambda_2 > 1$, suggesting that polymers are mostly stretched in the directions of $\boldsymbol{a}_1$ and $\boldsymbol{a}_2$, but coiled in other directions (this phenomenon will be interpreted later). To show how the polymers interact with the strain of the flow field intuitively, PDFs of $\cos\theta(\boldsymbol{e}_i, \boldsymbol{a}_i)$ at $t = 0.6$ s are shown in Fig. 5. It is shown that the directions of polymer conformation tend to be aligned with the corresponding strain directions of flow field and the PDF values around $\cos\theta(\boldsymbol{e}_i, \boldsymbol{a}_i) = 1$ are much larger, showing a strong relevance between the two tensors. At other instants the same phenomena are found but not shown here for brevity. Consider-

ing the alignment of the corresponding eigenvectors

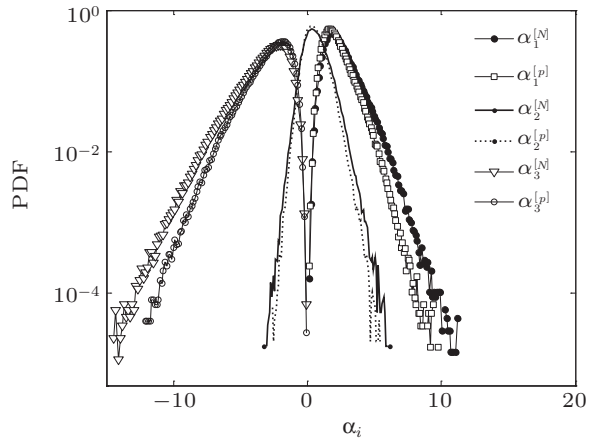


Fig. 3. PDFs of three eigenvalues for rate-of-strain tensor at $t = 0.6$ s.

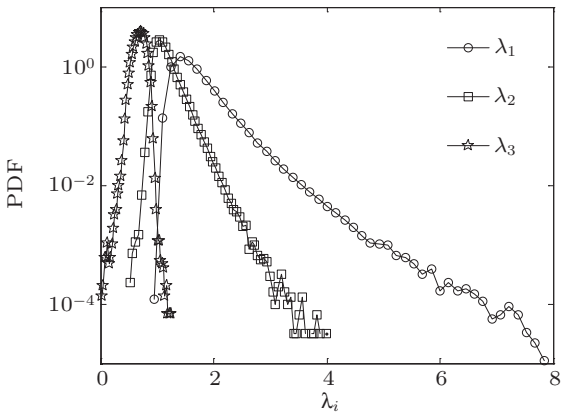


Fig. 4. PDFs of three eigenvalues for polymer conformation tensor at $t = 0.6$ s.

between the two tensors, obviously there should exist a strong relevance and consistency between the corresponding eigenvaules of these two tensors, which show the deformation strength of flow field and that of polymer conformation field, respectively. As given in Fig. 3, in the turbulence with polymer additives, α_1 and α_2 are positively skewed, which in some way indicates that λ_1 and λ_2 are skewed at $\lambda_1 > 1$ and $\lambda_2 > 1$, i.e., the polymers are mostly stretched in two directions in vortex sheets. On the other hand, it suggests that polymers play a more important role in vortex sheets.

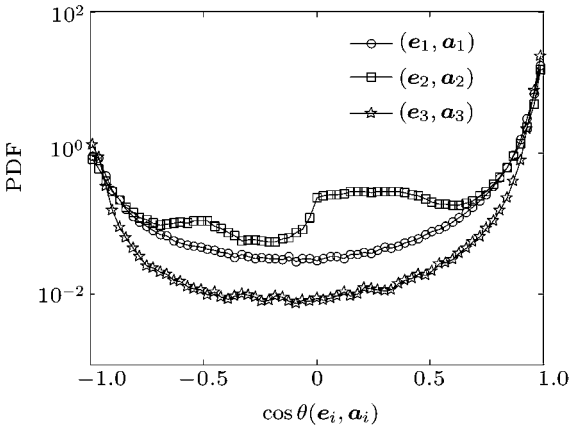


Fig. 5. PDFs of the cosine of the angle between $\boldsymbol{e}_i$ and $\boldsymbol{a}_i$ ($i = 1, 2, 3$) at $t = 0.6$ s for polymer solution flow.

To further show the contribution of polymers to the strain, we investigate the mean strain transport equation of DHIT with polymer additives:[24]

$$\frac{\partial\langle\mathbb{S}\rangle}{\partial t} = \underbrace{-\langle S_{ik}S_{kj}S_{ij}\rangle}_{\text{strain production}} \underbrace{-\frac{1}{4}\langle\omega_i\omega_j S_{ij}\rangle}_{\text{vortex stretching effect}} + \underbrace{\upsilon^{[s]}\langle S_{ij}\nabla^2 S_{ij}\rangle}_{\text{strain viscous dissipation}} + \underbrace{\left\langle \frac{\partial^2 T_{ik}^{[p]}}{\partial x_k \partial x_j} S_{ij} \right\rangle}_{\text{polymers effect}}, \tag{8}$$

where the operator $\langle\cdot\rangle$ denotes ensemble average, $\mathbb{S} = S_{ij}S_{ij}/2$ the total strain, $S_{\text{str}} = -S_{ik}S_{kj}S_{ij}$ the strain production from strain self-amplification, $W_{\text{str}} = \omega_i\omega_j S_{ij}/4$ the enstrophy production effect on the total strain, $V_{\text{str}} = \upsilon^{[s]}S_{ij}\nabla^2 S_{ij}$ the strain viscous dissipation, $Sp_{ij} = \partial^2 T_{ik}^{[p]}/\partial x_k \partial x_j$ the polymer effect tensor influencing the generation of strain, $p_{\text{str}} = Sp_{ij}S_{ij}$ the polymer effect due to the interaction between strain and polymer elastic stress (or polymer conformation) and does not appear in the Newtonian fluid case.

PDFs of strain $S_{ij}^{[p]}S_{ij}^{[p]}/2$ at sequential instants are shown in Fig. 6 for both the Newtonian fluid case and the polymer solution case. It is obtained that the addition of polymers leads to a remarkable decrease in the regions of large strain with only a few regions (near the origin) increased weakly. As is known, for both the Newtonian fluid case and the polymer solution case there is a strong positive correlation between strain generation and strain, i.e., the main source of the strain generation is its self-amplification.[25] In the previous study we found that for the polymer solution case, the polymer effect is negatively skewed, i.e., the presence of polymers can inhibit the strain generation.[24] Here, to make a comparison between the polymer effect and strain self-

amplification, joint PDF (JPDF) of $p_{\rm str}$ and $s^{[p]}_{\rm str}$ is shown in Fig. 7, which can be divided into four quadrants as follows: i) the first quadrant, in which $p_{\rm str} > 0$ and $s^{[p]}_{\rm str} > 0$, and both the polymer effect and the strain self-amplification contribute to the strain generation; ii) the second quadrant, in which $p_{\rm str} < 0$ and $s^{[p]}_{\rm str} > 0$, strain self-amplification contributes to the strain generation, but the polymer effect resists; iii) the third quadrant, in which $p_{\rm str} < 0$ and $s^{[p]}_{\rm str} < 0$, both the strain self-amplification and the polymer effect resist the strain generation; iv) the fourth quadrant, in which $p_{\rm str} > 0$ and $s^{[p]}_{\rm str} < 0$, the polymer effect contributes to the strain generation but the strain self-amplification resists. In DHIT with polymers (as shown in Fig. 7), JPDF of $p_{\rm str}$ and $s^{[p]}_{\rm str}$ mostly concentrates in the second and third quadrants, especially in the second quadrant, which implies that self-amplification is mostly conducible to strain generation but polymers mostly hold back the strain generation, thus increasing the "strain generation resistance" to flow structure. Besides, considering the amplitudes of two factors, we observe that the polymer effect $p_{\rm str}$ has a similar order of magnitude to that of the strain production $s^{[p]}_{\rm str}$, indicating that this effect is pronounced and can counteract a remarkable part of $s^{[p]}_{\rm str}$. In this way the strain in the polymer solution case can be suppressed, then the strain self-amplification is reduced, and so on. From the phenomenological viewpoint, the introduction of polymer additives inhibits the generation of vortex sheets, where strain dominates and most energy dissipation occurs. The results are validated by the visualization of vortex sheets on different scales (as shown in Fig. 2).

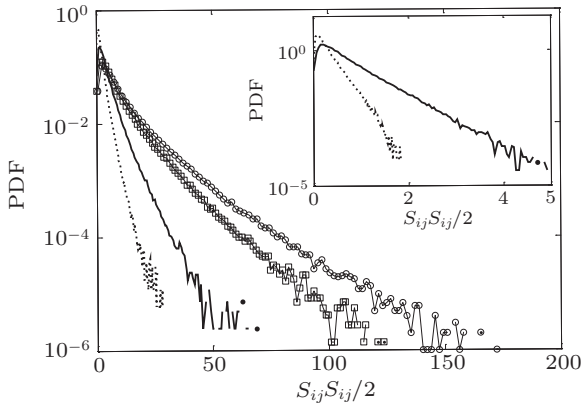


Fig. 6. PDFs of the strain in DHIT for Newtonian fluid and polymer solution cases. (○) Newtonian fluid case, (□) polymer solution case at $t = 0.6$ s, and the solid line for Newtonian fluid case, the dashed line for polymer solution case at $t = 2.0$ s; inset: the solid line for Newtonian fluid case, the dashed line for polymer solution case at $t = 5.0$ s.

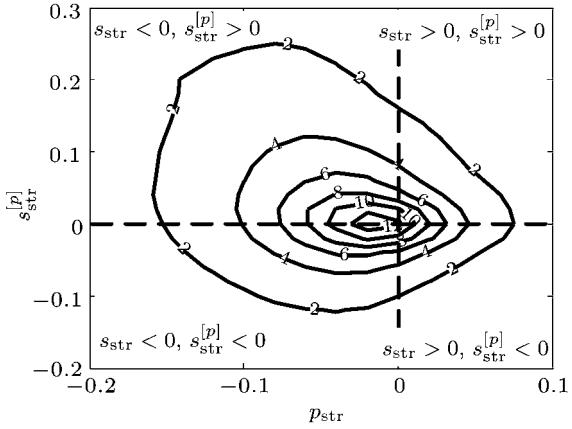


Fig. 7. $p_{\rm str}$ versus $s^{[p]}_{\rm str}$ for JPDF at $t = 0.6$ s in polymer solution case ($Wi = 0.62$, $\beta = 0.6$).

4.2.2. Interaction between polymers and vorticity

According to the above analyses, rate-of-strain tensor and polymer conformation tensors exhibit close correlation, and the strain generation is inhibited due to the interaction between polymers and strain, leading to the reduction of the strength of the vortex sheet, energy dissipation, and so on. Except for vortex sheets, vortex tubes related to vorticity also play an important role in turbulence and have also been found to be inhibited due to the presence of polymers as shown in Fig. 1. To obtain the inherent mechanism, we study the interaction between polymers and vorticity next.

Among the most basic question about the properties and dynamics in turbulent flows is the relation between vorticity vector and rate-of-strain tensor (geometric study). Several investigations on the Newtonian fluid turbulent flows have been carried out. For DHIT with polymers, the results are shown in Fig. 8, from which we can clearly see that the tendency towards the alignment between $\boldsymbol{e}_2$ and $\boldsymbol{\omega}$ is similar to that for the Newtonian fluid case, but some slight changes can be found. PDF values are reduced for the completely parallel and antiparallel cases, i.e., $\theta_1 = 0°$ (where θ_1 is the angle between $\boldsymbol{e}_2$ and $\boldsymbol{\omega}$) and $\theta_1 = 180°$. Besides, PDF value is slightly decreased for the completely vertical case (i.e. $\theta_1 = 90°$). At other instants the same phenomena are found but not shown here for brevity. Neglecting the variation of magnitude, in DHIT with polymers, the presence of polymers does not modify the shape of PDF, suggesting that it does not greatly influence the alignment characteristics of the relationship between vorticity vector and rate-of-strain tensor for Wi in our simu-

lation.

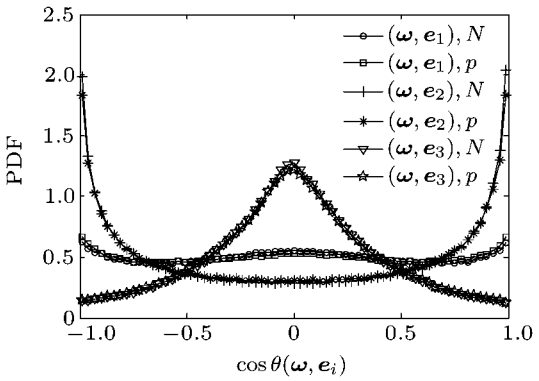


Fig. 8. PDFs of the cosine of the angle between $\boldsymbol{\omega}$ and $\boldsymbol{e}_i$ $(i = 1, 2, 3)$ at $t = 0.6$ s.

Likewise, the alignments between vorticity vector $\boldsymbol{\omega}$ and the three eigenvectors $(\boldsymbol{a}_i,\ i = 1, 2, 3)$ of polymer conformation tensor were investigated according to PDFs of $\cos\theta(\boldsymbol{\omega}, \boldsymbol{a}_i)$ at $t = 0.6$ s as shown in Fig. 9. The results show that vorticity vector tends to be aligned with the first and the intermediate eigenvectors of polymer conformation tensor and in the two directions along which polymers are mostly stretched with $\lambda_1 > 1$ and $\lambda_2 > 1$ (as shown in Fig. 4). At other instants the same phenomena are found but not shown here for brevity. This is similar to the result of alignment characteristics between vorticity vector and rate-of-strain tensor as shown in Fig. 8. Besides, the vorticity vector tends to be vertical to $\boldsymbol{a}_3$. The above results manifest a strong relevance between vorticity vector and polymer conformation tensor.

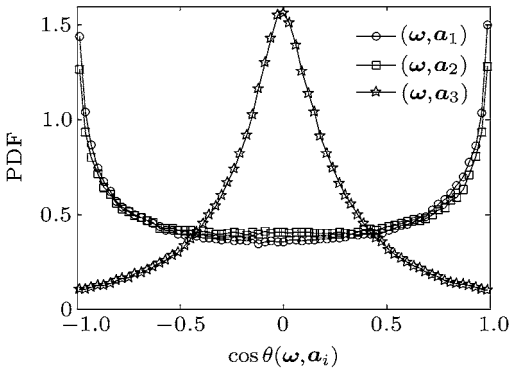


Fig. 9. PDFs of the cosine of the angle between $\boldsymbol{\omega}$ and $\boldsymbol{a}_i$ $(i = 1, 2, 3)$ at $t = 0.6$ s.

The enstrophy indicates the strength of vortex structure and is mainly generated by the stretching of vortex tubes, which is regarded as the impetus of turbulence maintenance. Therefore, in order to understand the interaction between polymers and vorticity more deeply we study the enstrophy transport equation of DHIT in the polymer solution case, as follows:[24]

$$\partial\Omega/\partial t = \underbrace{\langle\omega_i\omega_j S_{ij}\rangle}_{\text{enstrophy production}} - \underbrace{\upsilon^{[s]}\langle(\partial\omega_i/\partial x_j)^2\rangle}_{\text{enstrophy dissipation}} + \underbrace{\langle\omega_i(\partial^2 T^{[p]}_{mj}/\partial x_m\partial x_n)\varepsilon_{nji}\rangle}_{\text{polymers effect}}, \tag{9}$$

where ε_{nji} is the permutation symbol, ω_i the i-th component of vorticity vector $\boldsymbol{\omega} = \boldsymbol{\nabla}\times\boldsymbol{u}$, $\Omega = \omega_i\omega_i/2$ the enstrophy, $S_{\text{ens}} = \omega_i\omega_j S_{ij}$ the enstrophy production due to the interaction between vorticity and strain, $W_i = \omega_j S_{ij}$ the vortex stretching vector, $V_{\text{ens}} = \upsilon^{[s]}(\partial\omega_i/\partial x_j)^2$ the enstrophy viscous dissipation, $W_i^{[p]} = (\partial^2 T^{[p]}_{mj}/\partial x_m\partial x_n)\varepsilon_{nji}$ the polymer effect vector, and $p_{\text{ens}} = \omega_i W_i^{[p]}$ the polymer effect due to interaction between vorticity vector and polymer conformation tensor and does not appear in the Newtonian fluid case.

First, we show PDFs of the enstrophy in Fig. 10 at three sequential instants. Compared to its Newtonian counterpart, the addition of polymers leads to a decrease of the PDF value for the major part of large enstrophy and an increase of PDF value only in a narrow part near the origin. This phenomenon is more remarkable at $t = 2.0$ s and 5.0 s, which is similar to that for the strain (see Fig. 6).

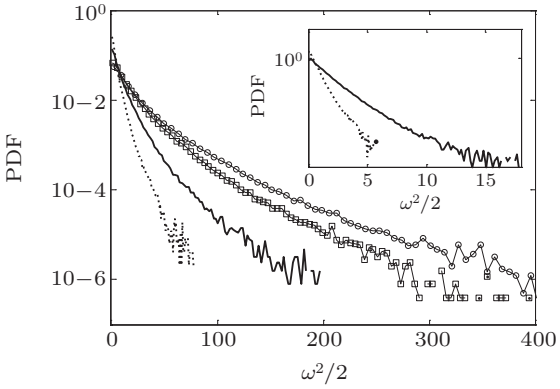


Fig. 10. PDFs of the enstrophy in DHIT for Newtonian fluid and polymer solution cases. (○) Newtonian fluid case, (□) polymer solution case at $t = 0.6$ s and the solid line for Newtonian fluid case, the dashed line for polymer solution case at $t = 2.0$ s; inset: the solid line for Newtonian fluid case, the dashed line for polymer solution case at $t = 5.0$ s.

Like self-amplification to strain, the enstrophy production term is very important for vorticity generation in the Newtonian fluid case and is found to be essentially positively skewed,[24] which is regarded as a consequence of the prevalence of the vortex stretching process over vortex compression. This irreversible tendency can be characterized locally by considering the PDF of the cosine of the angle between $\boldsymbol{\omega}$ and $\boldsymbol{W}$ as shown in Fig. 11(a). The PDF value of $\cos\theta(\boldsymbol{\omega}, \boldsymbol{W})$ is much larger in the region around $\theta_2 = 0°$ (where θ_2 is the angle between vectors of $\boldsymbol{\omega}$ and $\boldsymbol{W}$) than in the region around $\theta_2 = 180°$. In other words, there exists a strong tendency towards alignment between $\boldsymbol{\omega}$ and $\boldsymbol{W}$ in the strict sense, i.e., a tendency towards their being parallel but not antiparallel to each other, indicating that the vortex tubes are mostly stretched by $\boldsymbol{W}$. For the polymer solution case, shown in Fig. 11(a), the tendency is the same as that for the Newtonian fluid case with only a slight change for PDF value in the regions around $\theta_2 = 0°$ and $\theta_2 = 180°$, qualitatively similar to the experimental results of Liberzon *et al.*[13] It suggests that polymers would not change the characteristics of the interaction between $\boldsymbol{\omega}$ and $\boldsymbol{W}$. In DHIT with polymer additives, there also exists polymer conformation acting on the vortex tubes by $\boldsymbol{W}^{[p]}$. The relationship between $\boldsymbol{\omega}$ and $\boldsymbol{W}^{[p]}$ is also characterized locally by considering the PDFs of the cosine of the angle between them, as shown in Fig. 11(b). Contrary to the relation between $\boldsymbol{\omega}$ and $\boldsymbol{W}$, the PDF values of $\cos\theta(\boldsymbol{\omega}, \boldsymbol{W}^{[p]})$ in the region around $\theta_3 = 180°$ (where θ_3 is the angle between $\boldsymbol{\omega}$ and $\boldsymbol{W}^{[p]}$) are much larger than in the region around $\theta_3 = 0°$, at three different instants. With the angle $\theta_3$approaching to zero, the PDF value of $\cos\theta(\boldsymbol{\omega}, \boldsymbol{W}^{[p]})$ reduces quickly. It suggests that the polymer effect vector tends to be antiparallel to the vorticity vector, which compresses vortex tubes, thus inhibiting the generation of new vortex tubes especially on a small scale.

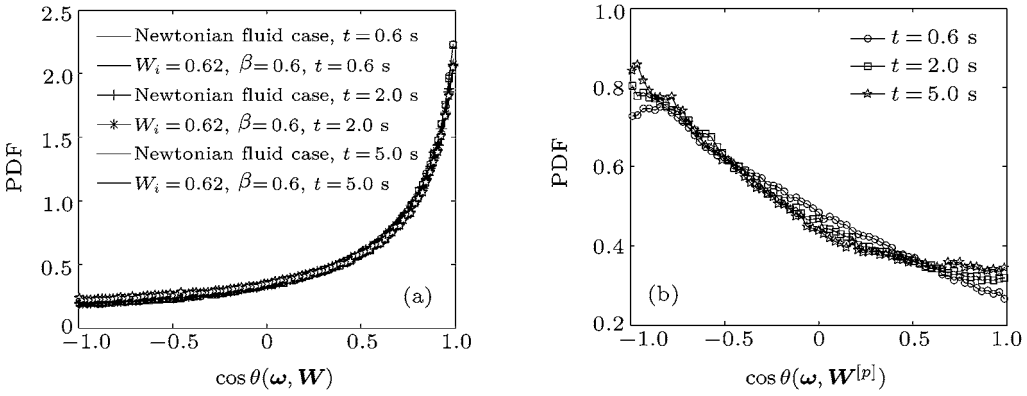


Fig. 11. (a) PDFs of the cosine of the angle between vorticity ($\boldsymbol{\omega}$) and vortex stretching vector ($\boldsymbol{W}$) for Newtonian fluid and polymer solution cases; (b) PDFs of the cosine of the angle between vorticity ($\boldsymbol{\omega}$) and polymer stretching or compressing vector ($\boldsymbol{W}^{[p]}$) for polymer solution case.

To further show the influence of the polymer effect $p_{\rm ens}$ on enstrophy production $s^{[p]}_{\rm ens}$, the JPDF at $t = 0.6$ s is shown in Fig. 12, which can similarly be divided into four quadrants as follows: a) the first quadrant, in which $p_{\rm ens} > 0$ and $s^{[p]}_{\rm ens} > 0$, and both polymer and vortex stretching vectors are parallel to vorticity vector, thus stretching the tubes and contributing to the vortex generation; b) the second quadrant, in which $p_{\rm ens} < 0$ and $s^{[p]}_{\rm ens} > 0$, and the vortex stretching vector contributes to the vortex generation, but polymer effect vector is antiparallel to vorticity vector, thus compressing the tubes and resisting the vortex generation; c) the third quadrant in which $p_{\rm ens} < 0$ and $s^{[\rm p]}_{\rm ens} < 0$, and both polymer and vortex stretching vectors resist the vortex generation; d) the fourth quadrant, in which $p_{\rm ens} > 0$ and $s^{[p]}_{\rm ens} < 0$, and the polymer effect vector contributes to the vortex generation, but vortex stretching vectors resist it. As shown in Fig. 12, in DHIT with polymers, the contributions of $s^{[p]}_{\rm ens}$ and $p_{\rm ens}$ mostly focus in the second quadrant, implying that vortex stretching vector tends to be conducible to the vortex generation but the polymer effect vector tends to increase the "stretching resistance" of vortex tubes. Besides, the amplitudes of the two factors are of the same order of magnitude, indicating a strong feedback of polymers on flow structure because of its elastic nature, and polymers almost counteract the effect of vortex stretching in DHIT with polymer

additives. Finally due to the elastic nature, the enstrophy (strength of vorticity) and its production (a source of turbulence maintenance) are undoubtedly reduced in the presence of polymers as compared with that of the Newtonian fluid case (Ref. [24]). From the phenomenological viewpoint, the introduction of polymer additives inhibits the generation of vortex tubes, where the vorticity is dominant. The results are validated by the visualization of vortex tubes on different scales (as shown in Fig. 1).

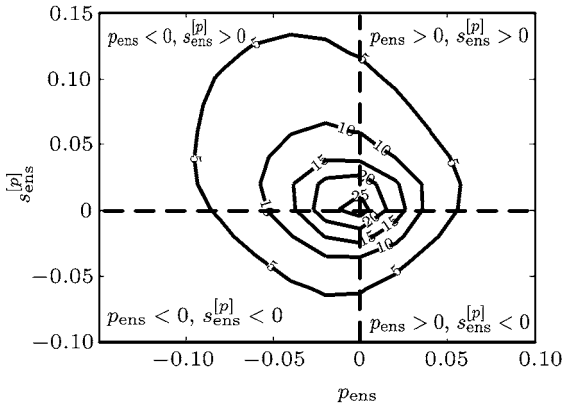


Fig. 12. $p_{\rm ens}$ versus $s^{[p]}_{\rm ens}$ for JPDF at $t = 0.6$ s in polymer solution case ($Wi = 0.62$, $\beta = 0.6$).

5. Conclusion and discussion

In order to understand the polymer effect or additive-turbulence interaction, we investigate the relationship between turbulence characteristics and the polymer conformation field by the DNS of DHIT with and without polymers. Through visualizing vortex tubes and sheets and investigating the interactions among polymer conformation tensor, vorticity vector, and rate-of-strain tensor, we can draw the following conclusions.

(I) There exists a remarkable inhibition of vortex structures in intermediate-scale and small-scale fields but not for large-scale field in DHIT with polymers, which can even terminate subsequent energy cascades to modify the turbulent features for the polymer solution case.

(II) In DHIT with polymers, the stretching and the compressing strengths of the flow field are weakened in all the directions determined by eigenvectors of the rate-of-strain tensor due to the polymer effect. The eigenvectors of the polymer conformation tensor tend to be aligned with those of the rate-of-strain tensor, implying a close relationship between them. Similar to flow structure, polymers are mostly stretched in two directions in vortex sheets, suggesting that polymers may have a strong feedback among these structures. As compared with its Newtonian counterpart, a reduction of strain is observed. Through plotting JPDF of the polymer effect term $p_{\rm str}$ versus the strain production term $s^{[p]}_{\rm str}$ in the mean strain transport equation of DHIT, it is obtained that during the strain generation, the polymer effect and strain self-amplification can be similar in order of magnitude but opposite in sign (negative for the former and positive for the latter), which increases "strain generation resistance" and inhibits the generation of vortex sheets, especially on a small scale.

(III) Analogous to the relationship between the vorticity vector and rate-of-strain tensor, the vorticity vector tends to be aligned with the first and the intermediate eigenvectors of the polymer conformation tensor, especially with the intermediate eigenvector. As compared with its Newtonian counterpart, a reduction of enstrophy is observed in DHIT in the presence of polymers. During its generation, the angle between the vorticity vector and vortex stretching vector it is skewed at 0°, but between the polymer effect vector and vorticity vector is skewed at 180°. Through plotting JPDF of the polymer effect term $p_{\rm ens}$ versus the enstrophy production term $s^{[p]}_{\rm ens}$ in the enstrophy transport equation of DHIT, it is obtained that $p_{\rm ens}$ and $s^{[p]}_{\rm ens}$ can be similar in order of magnitude but opposite in sign (the former is negative and the latter is positive), which straightforwardly increases "vorticity generation resistance" and inhibits the generation of vortex tubes, especially on a small scale.

In summary, our study suggests a strong relevance among vorticity vector, rate-of-strain tensor, and polymer conformation tensor, and the relevance inhibits the vorticity (or enstrophy) and strain generation, finally leading to the turbulence inhibition. It is noticeable that in spite of the existence of polymers the interaction between vorticity vector and rate-of-strain is unchanged. We believe that by establishing and studying their inherent relationships, the dynamics of the polymer solution, and the mechanism and phenomenon in turbulent drag-reducing flows can be further understood. Our long-term goal is to establish some methods associated with sub-grid modeling for large eddy simulation of turbulent drag-reducing flows by additives through a series of very detailed studies of the viscoelastic effect on turbulence, as done in this

paper. The present findings may contribute to this purpose.

Acknowledgments

We thank Prof. B. Yu of China University of Petroleum (Beijing) and Dr. Y. Yamamoto of Kyoto University, for their discussion on DNS. The authors are also very grateful for the enthusiastic help to all members of Complex Flow and Heat Transfer Laboratory of Harbin Institute of Technology.

References

[1] Toms B A 1949 *Proceedings of the First International Congress of Rheology* (Amsterdam: North Holland) p. 135
[2] Lumley J L 1973 J. *Polymer Sci. Macrom. Rew.* **7** 263
[3] Ptasinski P K, Boersma B J, Nieuwstadt F T M, Hulsen M A, van den Brule B H A A and Hunt J C R 2003 *J. Fluid Mech.* **490** 251
[4] Luchik T S and Tiederman W G 1988 *J. Fluid Mech.* **190** 241
[5] Den Toonder J M J, Hulsen M A, Kuiken G D C and Nieuwstadt F T M 1997 *J. Fluid Mech.* **337** 193
[6] Li F C, Kawaguchi Y, Hishida K and Oshima M 2006 *Exps. Fluids* **40** 218
[7] Sureshkumar R, Beris A N and Handler A H 1997 *Phys. Fluids* **9** 743
[8] Dimitropoulos C D, Sureshkumar R and Beris A N 1998 *J. Non-Newtonian Fluid Mech.* **79** 433
[9] Friehe C A and Schwarz W H 1970 *J. Fluid Mech.* **44** 173
[10] McComb W D, Allan J and Greated C A 1977 *Phys. Fluids* **20** 873
[11] van Doorn E, White C M and Sreenivasan K R 1999 *Phys. Fluids* **8** 2387
[12] Cadot O, Boon D and Douady S 1998 *Phys. Fluids* **10** 426
[13] Liberzon A, Guala M, Lüthi, Kinzelbach W and Tsinober A 2005 *Phys. Fluids* **17** 031707
[14] Liberzon A, Guala M, Kinzelbach and Tsinober A 2006 *Phys. Fluids* **18** 125101
[15] Crawford A M, Mordant N, Xu H T and Bodenschatz E 2008 *New J. Phys.* **10** 123015
[16] Ouellette N T, Xu H T and Bodenschatz E 2009 *J. Fluid Mech.* **629** 375
[17] Tabor M and de Gennes P G 1986 *Europhys. Lett.* **2** 519
[18] de Gennes P G 1986 *Physica* A **140** 9
[19] de Angelis E, Casciola C M, Benzi R and Piva R 2005 *J. Fluid Mech.* **531** 1
[20] Kalelkar C, Govindarajan R and Pandit R 2005 *Phys. Rev.* E **72** 017301
[21] Perlekar P, Mitra D and Pandit R 2006 *Phys. Rev. Lett.* **97** 264501
[22] Berti S, Bistagnino A, Boffetta G, Celani A and Musacchio S 2006 *Europhys. Lett.* **76** 63
[23] Jin S 2007 *Numerical Simulations of a Dilute Polymer Solution in Isotropic Turbulence* Ph. D. Thesis (New York: The Cornell University)
[24] Cai W H, Li F C and Zhang H N 2010 *J. Fluid Mech.* **665** 334
[25] Sagaut P and Cambon C 2008 *Homogeneous Turbulence Dynamics* (New York: Cambridge University Press) p. 112
[26] Taylor G I 1938 *Proc. Roy. Soc.* A **164** 15
[27] Kolmogorov A N 1941 *Dokl. Akad. Nauk SSSR* **30** 9; reprinted in *Proc. Roy. Soc. Lond.* A 1991 **9** 434
[28] Tennekes H and Lumley J L 1972 *A First Course in Turbulence* (Cambridge, Massachusetts: MIT Press) p. 103
[29] Tsinober A 2000 paper appearing in *Turbulence Structure and Vortex Dynamics* by Hunt J C R and Vassilicos J C (New York: Cambridge University Press) p. 164
[30] Siggia E D 1981 *J. Fluid Mech.* **107** 375
[31] Douady S, Couder Y and Brachet M E 1991 *Phys. Rev. Lett.* **67** 983
[32] Jimenez J, Wray A A, Saffman P G and Rogallo R S 1993 *J. Fluid Mech.* **255** 65
[33] Rogers M M and Moser R D 1994 *Phys. Fluids* **6** 903
[34] Robinson S K 1991 *Ann. Rev. Fluid Mech.* **23** 601
[35] Adrian R J, Meinhart C D and Tomkins C D 2000 *J. Fluid Mech.* **422** 1
[36] Chong M S, Perry A E and Cantwell B J 1990 *Phys. Fluids* **2** 765
[37] Chen J H, Chong M S, Soria J, Sondergaard R, Perry A E, Rogers M, Moser R and Cantwell B J *Proceedings of the* 1990 *CTR Summer Program*, Stanford, CA, 1990 p. 139
[38] Martín J, Ooi A, Chong M S and Soria J 1998 *Phys. Fluids* **10** 2336
[39] Nomura K and Post G 1998 *J. Fluid Mech.* **377** 65
[40] Soria J, Sondergaard R, Cantwell B J, Chong M S and Perry A E 1994 *Phys. Fluids* **6** 871
[41] Blackburn H, Mansour N and Cantwell B 1996 *J. Fluid Mech.* **310** 269
[42] Tsinober A 1998 *Eur. J. Mech.* B: *Fluids* **17** 421
[43] Ashurst W T, Kerstein A R, Kerr R M and Gibson C H 1987 *Phys. Fluids* **30** 2343
[44] Vincent A and Meneguzzi M 1991 *J. Fluid Mech.* **225** 1
[45] Tsinober A, Kit E and Dracos T 1992 *J. Fluid Mech.* **242** 169
[46] Jiménez J 1992 *Phys. Fluids* **4** 652
[47] Kawaguchi Y, Segawa T, Feng Z P and Li P W 2002 *Int. J. Heat and Fluid Flow* **23** 700
[48] Kim K, Li C F, Sureshkumar R, Balachandar S and Adrian R J 2007 *J. Fluid Mech.* **584** 281
[49] Kim K and Sirviente A I 2005 *Exps. Fluids* **38** 739
[50] Sibilla S and Beretta C P 2005 *Fluid Dyn. Res.* **37** 183
[51] Jeong J and Hussain F 1995 *J. Fluid Mech.* **285** 69
[52] Samanta G, Oxberry G, Beris A, Handler R and Housiadas K 2008 *J. Turbul.* **9** 1
[53] Cai W H, Li F C, Zhang H N, Li X B, Yu B, Wei J J, Kawaguchi Y and Hishida K 2009 *Phys. Fluids* **21** 115103
[54] Gyr A and Tsinober A 1996 *Proceedings of the Sixth European Turbulence Conference* Lausanne, Switzerland, 1996 p. 449
[55] Watanabe T and Gotoh T 2010 *Phys. Rev.* E **81** 066301
[56] Rogallo R S 1981 *Technical Report* No. 81315, NASA

[57] Canuto C, Hussaini M Y, Quarteroni A and Zang T A J 1988 *Spectral Methods in Fluid Dynamics* (New York: Spring-Verlag) p. 505

[58] Vaithianathan T, Robert A, Brasseur J G and Collins L R 2006 *J. Non-Newtonian Fluid Mech.* **140** 3

[59] Hunt J C R, Wray A A and Moin P 1988 *Center for Turbulence Research, Report CTR-S88* p. 193

[60] Perry A E and Chong M S 1987 *Ann. Rev. Fluid Mech.* **19** 125

[61] ZhouJ, Adrian R J, Balachandar S and Kendall T M 1999 *J. Fluid Mech.* **387** 353

[62] Abdel K W, Izawa S, Xiong A K and Fukunishi Y 2006 *Prog. Comput. Fluid Dyn.* **6** 403

[63] Alfonsi G and Primavera L 2009 *Flow Turbul. & Combust* **83** 61

[64] Dubief Y and Delcayre F 2000 *J. Turbul.* **11** 1

[65] Tanaka M and Kida S 1993 *Phys. Fluids* **5** 2079

[66] Horiuti K and Takagi Y 2001 *Phys. Fluids* **13** 3756

[67] Horiuti K and Takagi Y 2005 *Phys. Fluids* **17** 121703

[68] Moffatt H K, Kida S and Ohkitani K 1994 *J. Fluid Mech.* **259** 241

[69] Horiuti K, Takagi Y and Abe S 2006 *IUTAM Symposium on Elementary Vortices and Coherent Structures: Significance in Turbulence Dynamics* **79** p. 13

[70] da Silva C B and Pereira J C F 2008 *Phys. Fluids* **21** 055101